Computational Aspect of the Dual Reciprocity Method for Dynamics

S M Niku, R A Adey
Computational Mechanics BEASY
Ashurst, Southampton, UK.

1.0 Introduction

It is over twelve years since the dual reciprocity method (DRM) was first proposed by Nardini and Brebbia, [1]. Many authors have proposed extensions to the technique and it has been applied to dynamic problems, transient problems and others to transform equations to the boundary where the fundamental solution is now known. The technique provides a very general methodology for obtaining a boundary element solution to a wide range of problems [2].

Although a large amount of research has been devoted to the DRM, its impact in practical problem solving has been limited. The authors believe this has been due to two factors. The computational cost of the technique. For example, the computation of a general DRM term involves 3 matrix multiplication and an inversion. This requires 13 $N^3/3$ operations where N is the number of equation. In contrast, the direct solution of a system of equation requires $N^3/3$ operation. Thus the cost of using the DRM to transform the equation to the boundary is at least thirteen times more costly than solving the system of equations. (Note this is a minimum estimate as in many cases the cost is higher.)

The second factor is the reliability of the technique. For example, many authors have proposed the use of internal poles or points inside the domain. While this has been proved to be an effective solution strategy, the problem remains of deciding on the number and the position where the poles should be placed. Scheur & Adey [3] proposed an adaptive technique to solve this problem but this was only partially successful as it was discovered that the equation became nearly singular as the number of internal poles became large compared with the number of nodes on the boundary.

In this paper, the authors attempt to address the first point by reporting the results of some numerical experiments. The objective being to reduce the computational cost of the boundary element solution of problem where a fundamental solution is not known.

2.0 Dual Reciprocity Applied to Dynamics

The dual reciprocity method has been shown to provide an effective solution to computing the natural modes of vibration of elastic bodies without the presence of internal poles. [4]. Providing the objective is to compute the lower modes of vibration the technique is accurate without internal poles. However, the accuracy deteriorates significantly for the higher modes. In this case internal poles will be necessary.

3.0 Theory

The DRM is applied to the elasticity equation as follows.

3.1 General Vibration Problems

The conditions of equilibrium for elasto-dynamic problem interims displacement field in the absence of body forces can be expressed by:

$$\int(u) = GU_{K,jj} + \frac{G}{(1-2\nu)}U_{j,jK} = \rho\ddot{u}_K \qquad (1)$$

where ν is Poisson’s Ratio

G is the Shear Modulus

$$G = \frac{E}{2(1+\nu)}$$

E is the Modulus of Elasticity

ρ is the mass density

The boundary integral equation for this problem using the static fundamental solution is given by:

$$C^i_{lk}u^i_k = \int_\Gamma u_{lk}t_k d\Gamma - \int_\Gamma t_{lk}u_k d\Gamma - \rho\int_\Omega u_{lk}\ddot{u}_k d\Omega \qquad (2)$$

where

u and t are boundary displacements and tractions

u* and t* are Kelvin displacement and traction fundamental solutions and given by:

for 2D:

$$\begin{cases} u_{ij}^* = \dfrac{1}{8\pi(1-\nu)G} & \left[\left(3-4\nu\right)\delta_{ij} ln\left(\dfrac{1}{r}\right) + r_{,i}r_{,j}\right] \\ t_{ij}^* = \dfrac{-1}{4\pi(1-\nu)r} & \left[(1-2\nu)\delta_{ij} + 2r_{,i}r_{,j}\right]\dfrac{\delta r}{\delta n} - (1-2\nu)(r_{,i}n_j - r_{,j}n_i)\right] \end{cases} \tag{2.1}$$

and

for 3D:

$$\begin{cases} u_{ij}^* = \dfrac{1}{16\pi(1-\nu)Gr} & [(3-4\nu)\delta_{ij} + r_{,i}r_{,j}] \\ t_{ij}^* = \dfrac{-1}{8\pi(1-\nu)r^2} & \left[1-2\nu)\delta_{ij} + 3r_{,i}r_{,j}\ \right]\dfrac{\delta r}{\delta n} - (1-2\nu)(r_{,i}n_j - r_{,j}n_i)\right] \end{cases} \tag{2.2}$$

The boundary integral equation (2) requires to evaluate a volume integral involving the acceleration term $\ddot{u}$ and therefore is not practical to be used in the present form.

Using DRM, the acceleration term can be approximated by a series of geometric and time functions f and α

$$\ddot{u}_k(x, y, z, t) \cong \sum_{i=1} f^j(x, y, z)\alpha_K^j(t) \tag{3}$$

By taking geometric points (x,y,z) to nodal points one can express the general time variable α in terms of nodal acceleration

$$\underset{\sim}{\alpha} = \underset{\sim}{F}^{-1}\underset{\sim}{\ddot{U}} \tag{4}$$

substituting (3) into (2) one can obtain

$$C_{iK}^i u_K^i = \int_\Gamma u_{lK}^* t_K d\Gamma - \int_r t_{lK}^* u_K d\Gamma - \rho \sum_{i=1} \int (u_{lK}\hat{t}^j_{mK} - t_{lK}\hat{u}^j_{mK}) d\Gamma \alpha_K^j \tag{5}$$

where $\hat{u}^j$ & t^j are the displacements and tractions particular solutions to the equation $\rfloor(u) = f^j$(x,y,z).

The approximate function f(x,y,z) = (1+r) was used in this work, which is recommended by (Ref

1, 2 & 4).

The corresponding particular solutions are (Ref 4).

for 2D:

$$\hat{u}_{mK} = \frac{1-2\nu}{(5-4\nu)G}r_{,m}r_{,K}r^2 + \frac{1}{30(1-\nu)G}\left[\left(3-\frac{10\nu}{3}\right)\delta_{mK} - r_{,m}r_{,K}\right]r^3$$

$$\hat{t}_{mK} = \frac{2(1-2\nu)}{5-4\nu}\left[\frac{1+\nu}{1-2\nu}r_{,m}n_K + \frac{1}{2}r_{,K}n_m + \frac{1}{2}\delta_{mK}\frac{\delta r}{\delta n}\right]r + \frac{1}{15(1-\nu)} \tag{5.1}$$

$$\left[(4-5\nu)r_{,K}n_m - (1-5\nu)r_{,m}n_K + [(4-5\nu)\delta_{mK} - r_{,m}r_{,K}\ ]\frac{\delta r}{\delta n}\right]r^2$$

for 3D:

$$\hat{u}_{mK} = \frac{(1-2\nu)}{(6-4\nu)G}r_{,m}r_{,K}r^2 + \frac{1}{48(1-\nu)G}\left[\ \frac{11}{3} - 4\nu)\delta_{mK} - r_{,m}r_{,K}\right]r^3$$

$$\hat{t}_{mK} = \frac{(1-2\nu)}{3-2\nu}\left[\frac{1+2\nu}{1-2\nu}r_{,m}n_K + \frac{1}{2}r_{,K}n_m + \frac{1}{2}\delta_{mK}\frac{\delta r}{\delta n}\right]r + \frac{1}{24(1-\nu)} \tag{5.2}$$

$$\left[(5-6\nu)r_{,K}n_m - (1-6\nu)r_{,m}n_K + \left[(5-6\nu)\delta_{mK} - r_{,m}r_{,K}\right]\frac{\delta r}{\delta n}\right]r^2$$

Now by discretising the boundary and expressing (5) in a matrix form

$$\underset{\sim}{H}\underset{\sim}{U} - \underset{\sim}{G}\underset{\sim}{T} = -\rho(\underset{\sim}{H}\underset{\sim}{\hat{U}} - \underset{\sim}{G}\hat{T})\underset{\sim}{\alpha} \tag{6}$$

and substituting (4) into (6) gives

$$\underset{\sim}{H}\underset{\sim}{U} - \underset{\sim}{G}\underset{\sim}{T} = -\rho(\underset{\sim}{H}\underset{\sim}{\hat{U}} - \underset{\sim}{G}\hat{T})\underset{\sim}{F}^{-1}\underset{\sim}{\ddot{U}} \tag{7}$$

where $\hat{U}$ & $\hat{T}$ are Particular Solution Matrices.

In the original DRM formulation by Nardini & Brebbia and subsequent work (Ref 2 & Ref 4) the equation (7) is partitioned into two parts with respect to the boundary condition types and then condensed in order to eliminate D.O.F. with unknown tractions and express the final equation in terms of unknown displacement. In this work the implementation and computational complexity of the static condensation is avoided by multiplying both sides of equation (7) by G^{-1} and rearterms of unknown displacement. In this work the implementation and computational complexity of the static condensation is avoided by multiplying both sides of equation (7) by G^{-1} and rearranging which gives

$$\underline{K}\underline{U} + \underline{M}\ddot{\underline{U}} = \underline{T} \tag{8}$$

where

$$\underline{K} = \underline{G}^{-1}\underline{H} \tag{8.1}$$

and

$$M = -\rho\,(\underset{\sim}{K}\underset{\sim}{\hat{U}} - \underset{\sim}{\hat{T}})\,\underset{\sim}{F}^{-1} \tag{8.2}$$

It is interesting to note that this formulation now is very similar to the classic form obtained by the Finite Element Method and that K and M represent a form of distributed stiffness and mass matrix.

Assuming now that $U = \bar{U}$ on Γ_1 and $T = \bar{T}$ on Γ_2 one can partition equation (8) into:

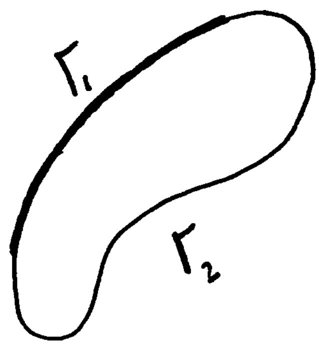

$$\begin{bmatrix} K_{11} & K_{12} \\ K_{21} & K_{22} \end{bmatrix}\begin{bmatrix} U_1 \\ U_2 \end{bmatrix} + \begin{bmatrix} M_{11} & M_{12} \\ M_{21} & M_{22} \end{bmatrix}\begin{bmatrix} \ddot{U}_1 \\ \ddot{U}_2 \end{bmatrix} = \begin{bmatrix} T_1 \\ T_2 \end{bmatrix} \tag{9}$$

The problem can now be solved directly in terms of U_2 without a need for static condensation, simply by rearranging the second equation in (9)

$$K_{22}U_2 + M_{22}\ddot{U}_2 = T_2 - (K_{21}U_1 + M_{21}\ddot{U}_1) \tag{10}$$

Another advantage of using the modified form given by (8) is the simplicity involving multi-zone problems.

By partitioning each zone system of matrices
in terms of external and internal
D. O. F., one can write

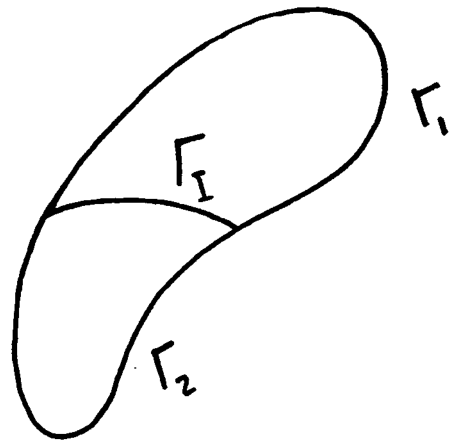

Zone 1:

$$\begin{bmatrix} K_{11} & K_{1I} \\ K_{I1} & K_{II}^{1} \end{bmatrix} \begin{bmatrix} U_1 \\ U_I^1 \end{bmatrix} + \begin{bmatrix} M_{11} & M_{1I} \\ M_{I1} & M_{II}^{1} \end{bmatrix} \begin{bmatrix} \ddot{U}_1 \\ \ddot{U}_I^1 \end{bmatrix} = \begin{bmatrix} T_1 \\ T_I^1 \end{bmatrix} \tag{10.1}$$

Zone 2:

$$\begin{bmatrix} K_{22} & K_{2I} \\ K_{I2} & K_{II}^{2} \end{bmatrix} \begin{bmatrix} U \\ U_I^2 \end{bmatrix} + \begin{bmatrix} M_{22} & M_{2I} \\ M_{I2} & M_{II}^{2} \end{bmatrix} \begin{bmatrix} \ddot{U}_2 \\ \ddot{U}_I^2 \end{bmatrix} = \begin{bmatrix} T_2 \\ T_I^2 \end{bmatrix} \tag{10.2}$$

Now assuming continuity of interface

$$\begin{cases} U_I^1 = U_I^2 = U_I \\ \ddot{U}_I^1 = \ddot{U}_I^2 = \ddot{U}_I \\ T_I^1 = T_I^2 = T_I \end{cases}$$

One can now simply substitute T_I^2 from (11.2) and substitute into (11.1) which will lead to the global equation for multi-zone problems.

3.2 Free Vibration Problems

The formulation for free vibration problems can be derived from equation (10) by setting the external leads to zero.

$$K_{22}U_2 + M_{22}\ddot{U}_2 = o \tag{12}$$

Assuming that the solution is time harmonic, one can write:

$$\ddot{U}_2 = -\omega^2 U_2 \tag{12.1}$$

Substituting (12.1) into (12) and rearrange

$$(K_{22} - w^2 M_{22})U_2 = o \tag{13}$$

which can be converted to the classical eigenvalue form by

$$(\underset{\sim}{A} - \lambda \underset{\sim}{I})U_2 = o \tag{14}$$

where

$$A = M_{22}^{-1}K_{22} \tag{14.1}$$

and

$$\lambda = \omega^2 \tag{14.2}$$

4.0 Computational Aspects

The computational costs for setting up free vibration system of matrices can be broken down as follows:

- **Computational Costs of K**

  This involves one inversion - multiplication as shown by (8.1) at total cost of $4N^3/3$ operation.

- **Computational Costs of M**

  This requires one matrix inversion and two multiplications as shown by (8.2) at total cost of $N^3 + N^3 + 4N^3/3 = 10N^3/3$.

- **Computational Costs of M^{-1} x K**

  This involves one inversion - multiplication as required by (14.1) at total cost of $4N^3/3$.

Please note that these ignore the cost of computing $\hat{\underset{\sim}{U}}$ and the addition involving $\underset{\sim}{K}\underset{\sim}{U} - \underset{\sim}{T}$ and that the cost of calculating $\underset{\sim}{K}$ has been taken into account once.

Therefore the total computational costs before solving the equations stands at $6N^3$. Considering the cost of solving a set of N series equation using direct technique is $N^3/3$. Therefore the cost of this analysis compared with standard static analysis is of the factor of 18 times higher which is currently unacceptable for industrial applications.

Back to Physics

It is well known from Structural Mechanics that quite accurate solutions can be obtained from lumped mass systems. This technique transforms the distributed mass matrix M into a diagonal matrix by adding the terms of the matrix to the diagonal. (Ref 7).

If $\underset{\sim}{M}$ is assumed to be a diagonal matrix could $\underset{\sim}{F}$ be assumed to be diagonal. This has a physical meaning. By assuming that F is diagonal, we are assuming that the acceleration of the source node under consideration is equation (2). Note that this does not mean that acceleration is assumed to be constant. Furthermore, if $\underset{\sim}{F}$ is diagonal could $\hat{\underset{\sim}{U}}$ and $\hat{\underset{\sim}{T}}$ be assumed to be diagonal.

Obviously, substantial savings can be made in the computational cost if assumption of this type can be made.

5.0 Observations

In order to study the reliability of simplifications of the mass matrix the following alternatives were considered to solve a variety of problems:

i) Solution based on diagonalising F only
ii) Solution based on diagonalising F, $\hat{U}$ and $\hat{T}$
iii) Solution based on diagonalising M only
iv) Solution based on diagonalising F and M only
v) Solution based on diagonalising F, $\hat{U}$, $\hat{T}$ and M.

The tests carried out consistently confirmed that options (iii) and (iv) produce reasonably accurate results for lower modes and the solution from these three options are very close. Options (ii) and (v) however consistently fail to produce any sensible solutions. All observations suggest that an optimum option is option (iv) by which both F and M are diagonalised.

Assuming that this option is adapted then the calculation for setting up the matrices before the eigenvalue solver would only involve two NxN matrix multiplication to evaluate K and $K\hat{U}$ which in total requires $2N^3$ operation. This is significantly lower than the figure of $6N^3$ which is required to carry out the full matrix analysis.

6.0 Test Cases

The objective of the tests was to determine the results of making assumptions of the form of the M matrix. In each case various simplifications have been applied.

Example 1 : Free Vibration of a Cantilevered Tapered Membrane

In this example, free vibration of a tapered membrane which clamped at the thicker end is studied.

The geometry and Boundary Element model of the problem is shown in Figure (5.1). The material properties given are

$E = 200 \times 10^9$ N/m^2 , n = 0.3 , r = 8000 kg/m^3

Table 1 Natural Frequencies of the Tapered Membrane using Different Strategies

Cantilevered TaperedMembrane			**Diagonalised Systems**				
Modes	**NAFEMs**	**DRM**	**F**	**F&U&T**	**F&U&T& M**	**M**	**F&M**
1	**280.37**	**279.79**	**339.03**	**220.171**	**230.61**	**268.031**	**272.49**
2	**817.00**	**800.22**	**1190.98**	**753.78**	**677.90**	**763.93**	**776.86**
3	**1022.27**	**1040.87**	**Illegal**	**981.89**	**842.86**	**982.83**	**1001.99**
4	**1545.98**	**1614.58**	**Illegal**	**1673.95**	**1226.03**	**1393.09**	**1413.08**
5	**2386.98**	**2542.91**	**Illegal**	**3687.39**	**1551.94**	**2037.27**	**2065.65**

Table 1 shows the solution given by Ref (6) and those obtained using DRM with 24 quadratic elements. A good comparison is observed between DRM and NAFEM's results Ref (6).

The table also shows a comparison between the natural frequencies obtained using original matrices and those using diagonalised systems. The mode shapes obtained are shown by Figures (2) which agree well with those from NAFEMs.

The examinations of the results revealed that the best results are obtained by diagonalising M or M and F matrices. The results using diagonalisation to take into account different direction produced poor results and the option was therefore eliminated. Diagonalising F or F&U&T or F&U&T&M

for this and other tests which were carried out produced poor results.

Based on these results it was decided to continue the experiment for more complex problems using diagonalise M and (M&F) systems only.

Example 2 : Free Vibration of a Long Cantilever Beam

This is an example of cantilever of length 1^{m} and depth 0.02^{m} (Fig). The material properties are assumed to be $\upsilon = o$ $E=1\ N/m^2$ $\rho = 1\ kg/m^3$.

The theoretical solution for the axial mode natural frequencies for a one dimensional beam is given by Ref (15).

$$W_n = \frac{R}{L}\left(n - \frac{1}{2}\right)\sqrt{\frac{E}{\rho}}$$

where L is the length of the beam

n is the number of axial modes.

Table 2 shows the natural frequencies associated with the first six modes. A very good comparison is observed between results using DRM for the axial mode which is the sixth mode in the table. (The first five modes are bending modes.)

The table also shows that again as previous example reasonable results have been produced using diagonalised M and F&M systems. The boundary element model and the bending modes of vibration are shown by Figures (3) and (4).

Table 2 Natural Frequencies of Thin Cantilever Beam

Thin Cantilever Beam			**Diagonalised Systems**	
Modes	**Analytical (Ref5)**	**DRM**	**M**	**F&M**
1	**-**	**0.02028**	**0.02818**	**0.02007**
1	**-**	**0.12660**	**0.12653**	**0.12765**
3	**-**	**0.35324**	**0.35282**	**0.35464**
4	**-**	**0.68856**	**0.68701**	**0.68981**
5	**-**	**1.13130**	**1.12700**	**1.13104**
6	**1.571**	**1.57060**	**1.57070**	**1.57430**

Example 3 : Free vibration of a Hollow Membrane Disc

In this example, free vibration of a hollow disc with internal and external radius of 1.8^{m} and 6.0^{m} is investigated. The material properties used are

$$E = 200 \times 10^{9} N\backslash \mathrm{m}^{2} \quad \nu = 0.3 \;\; \textit{and} \;\; \rho = 8000 kg\backslash \mathrm{m}^{3}$$

Solution for modes and natural frequencies of this problem is given by Ref (6). Table 2 shows the results obtained using DRM and diagonalised M and F matrices.

Again there is a good agreement between lower natural frequencies obtained using DRM and these given by NAFEMs (Ref 6).

In this case it is interesting to note that there is a shift in frequencies using diagonalised system.

It appears that the diagonalised techniques produced results close to full DRM, however there are additional fictitious modes created. This may be due to the fact that the disc was modeled by applying restraint at one point rather than modeling it as a free disc causing local perturbation of solution near the restraint node.

The modes of vibrations using full DRM are shown in Figure (5) which agree well with Ref (6).

Table 3 Natural Frequencies for Hollow Disc

Hollow Disc			**Diagonalised Systems**	
Modes	**NAFEMS**	**DRM**	**M**	**F&M**
4 & 5	**812.00**	**874.45**	**821.50**	**817.22**
6	**1421.00**	**1403.20**	**1118.38**	**1109.43**
7 & 8	**1474.90**	**1489.11**	**1199.50 1331.02**	**1186 1322.10**
9 & 10	**1662.85**	**1847.60**	**1459.04 1487.02**	**1441.74 1476.40**

Hollow Disc			Diagonalised Systems	
11 & 12	2114.96	2194.94	1518.63 1545.06	1505.30 1523.60
13 & 14	2367.37	2943.1	1863.89 1899.61	1838.22 1844.93

Example 4 : Free Vibration of a Micro Accelerometer Hinge

This is an example of a micro structure device. The device is a hinge used in an accelerometer.

The geometry is shown in Figure (6). The material properties used were assumed to be E=p=1 and υ=0.3.

Table 4 presents the natural frequencies using different lumping techniques.

Again it can be observed that results obtained by lumping M is in good agreement with that obtained using full matrices. The results obtained using lumped M&F also produce results with around 2-9% error. (Note. An interesting point is the results for the higher frequencies is quite good.)

Table 4 Natural Frequencies for accelerometer hinge

Micro	Hinge	Diagonalised	Systems
Mode	DRM	M	M&F
1	0.6674 e-03	0.66469 e-03	0.616726 e-03
2	0.143743 e-01	0.144512 e-01	0.139726 e-01
3	0.99003 e-01	0.97141 e-01	0.89130 e-01
4	0.19817 e+00	0.19290 e+00	0.184957 e+00
5	0.38349 e+00	0.357617 e+00	0.349093 e+00
6	0.59942 e+00	0.57347 e+00	0.549184 e+00

Example 5 : Free Vibration of a Clamped Lug

In this example, the free vibration of a three dimensional clamped lug is investigated. The geometry of this problem is shown by Figure (8).

The DRM and FE solution for the equivalent two dimensional version of this problem with linearised geometry is given by Ref (4).

The results obtained are shown in Table (5). Considering that in this analysis quadratic curved elements are used, good agreement can be observed with FE results based on flat elements given by Ref (6).

Again results based on diagonalised M and($\underset{\sim}{F}$ & $\underset{\sim}{M}$) seems to produce results which agrees well with the original DRM solution.

The boundary element model used for this analysis and the modes of vibration obtained are shown by figures (8).

Table 5 Results for Clamped Lug

Clamped Lug			**Diagonalised Systems**	
Modes	Ref (4)	DRM	**M**	$\underset{\sim}{F}$ & $\underset{\sim}{M}$
1	**1826**	**1793.95**	**1767.99**	**1778.43**
2	**3807**	**3734.04**	**3678.83**	**3701.12**
3	**3963**	**3858.86**	**3884.92**	**3925.99**

7.0 Summary

The results suggest that the technique for “lumping” or making diagonal the M matrix can be used to substantially reduce the cost of the DRM. Diagonalising the M and F maxtrix can provide quite accurate results and reduces the computational cost. The authors are aware that these examples do not comprehensively verify the idea and that more work needs to be done to i) establish the generality of the method and ii) establish a more robust mathematical basis for the technique.

The computational benefits are high. Lumping M reduces the costs by 4 $N^3/3$. Diagonalising M and F reduces the cost by $4N^3$ with corresponding reduction in Input Output costs and memory.

Further work is necessary to establish a clear mathematical basis. For example, similar reductions in the computation cost could be achieved by choosing a ***f*** function with a very local influence, ie with a very short decaying distance from the node.

Finally a completely different approach could be possible by attempting to generate the M matrix directly without regard to the BEM or DRM.

8.0 Acknowledgments

The authors wish to acknowledge the collaboration of Dr Luiz Wrobel, Tim Bridges and Dr Henry Power of WIT. The work was supported under the MASS project under the ESPRIT programme of the European Union. Partners in the project are Computational Mechanics BEASY, Wessex Institute of Technology, Microparts GMBH, and Technical University of Berlin.

9.0 References

1. Nardini D and Brebbia CA

A new approach to free vibration analysis using boundary elements, in proc 4th Int Conference, Boundary Elements, Computational Mechanics publications, Southampton and Springer Verlag, Berlin 1982.

2. Partridge, P W, Brebbia, C A and Wrobel, L C
The Dual Reciprocity Boundary Element Method, Computational Mechanics Publications, Southampton, and Elsevier, London 1992.

3. Schclar, N.A. and Adey, R.A.
"Adaptive Dual Reciprocity Boundary Element Method"
Boundary Element XIV Eds C.A. Brebbia, J. Domingues and F. Paris, Vol.1, 679-694, 1992.

4.) Bridges, T.R. & Wrobel, L.C.
"One the Calculation of Natural Frequencies of Microstructures using DRBEM".
Boundary Element Method XVI Conference, Southampton, UK, 12-15 July 1994.

5.) Craig, R.R.
Structural Dynamics, John Wiley, Chichester, 1981.

6. Abbasian, F, Dawswell, D J and Knowles, N C.
"Selected Benchmarks for Natural Frequency Analysis". NAFEMS Nov 1987.

7. Zlinkiewicz, O.C.
"The Finite Element Method".
Third Edition, ISBN 0-07-084072-5, McGraw Hill, U.K. 1977.

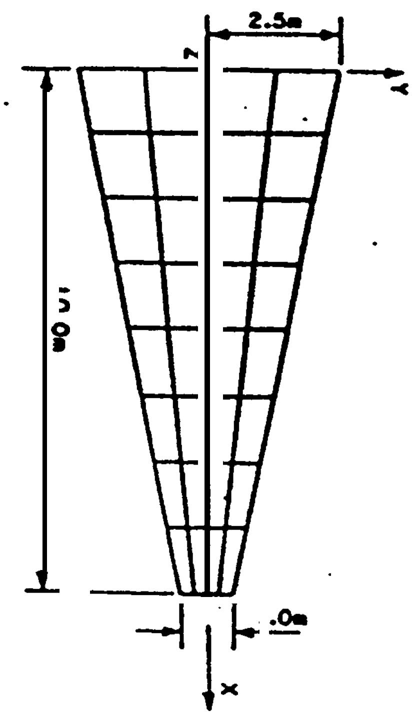

Figure 1.1

Fig (1.2)

Load set 1

BOUNDARY ELEMENT MODEL OF CANTILEVER TAPERED MEMBRANE

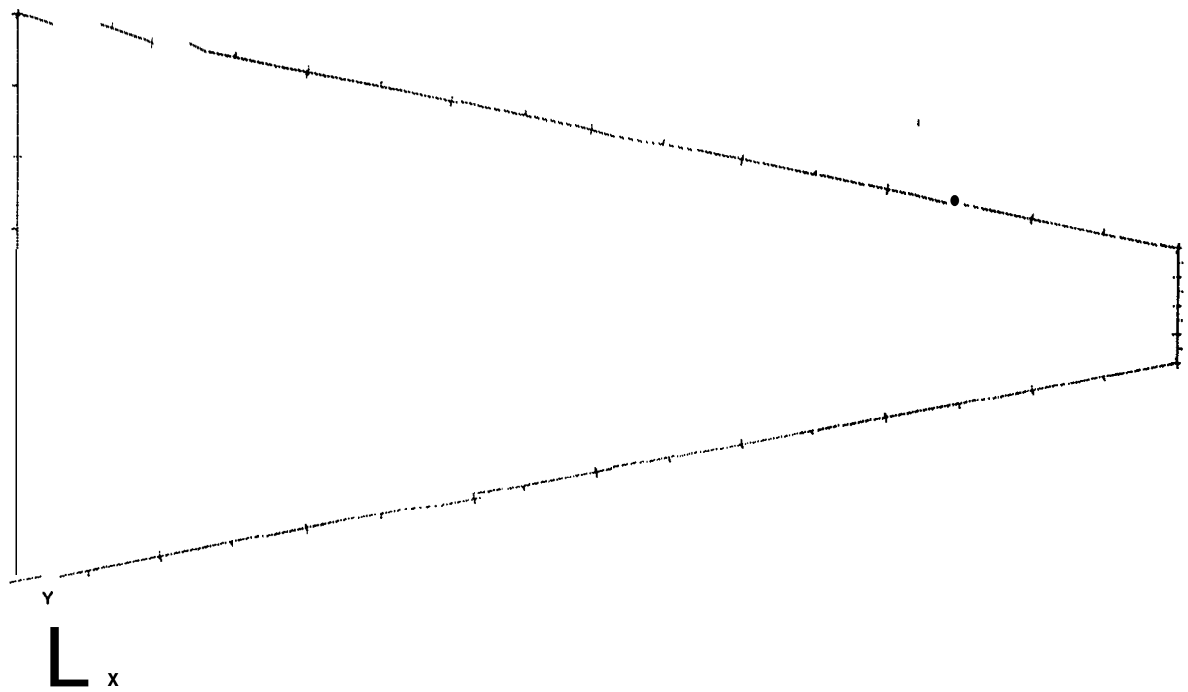

Fig (1.2)

5? {7"})

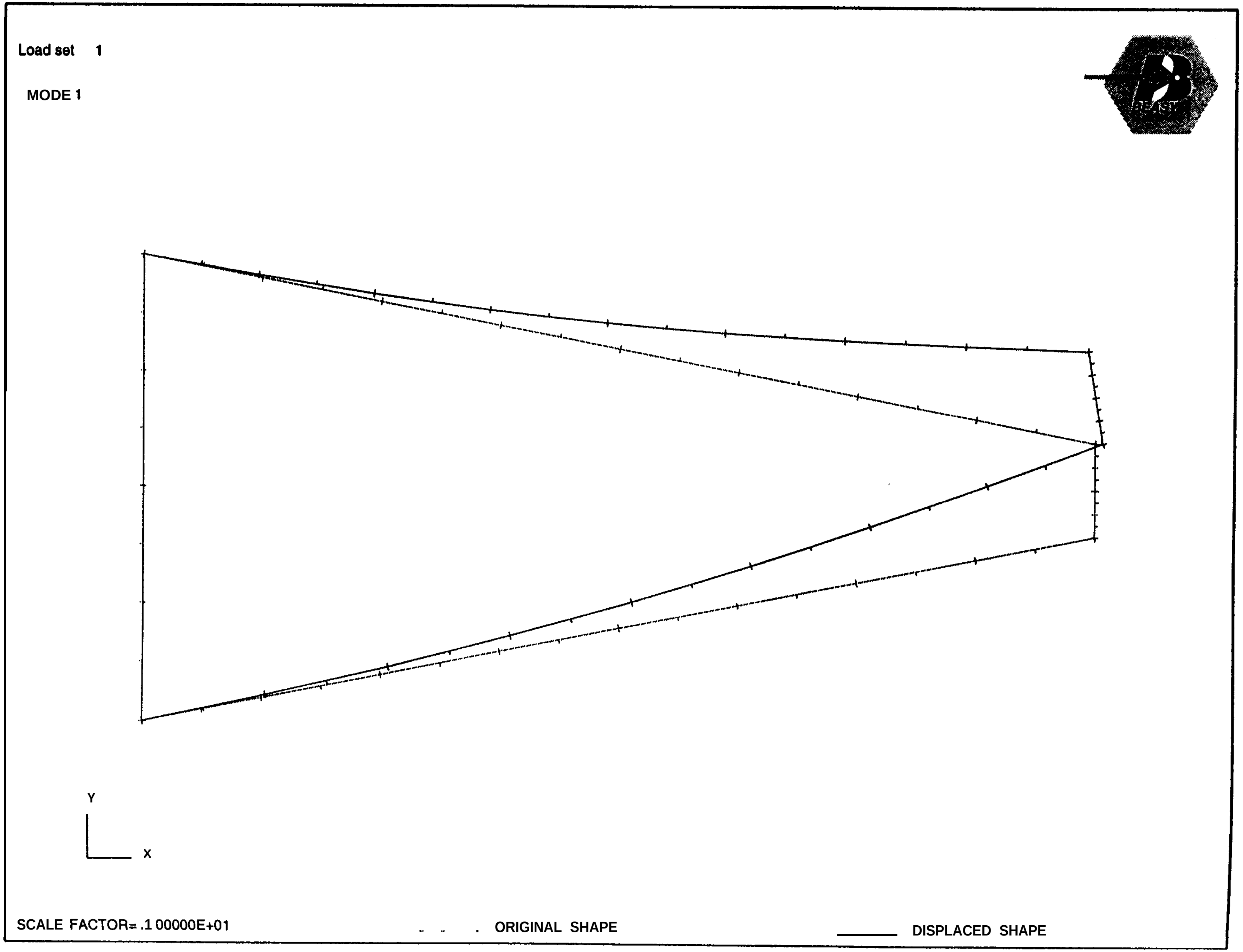
Load set 1
MODE 1
Y
X
SCALE FACTOR= .1 00000E+01
ORIGINAL SHAPE
DISPLACED SHAPE

Fig (2.1)

Fig (7.2)

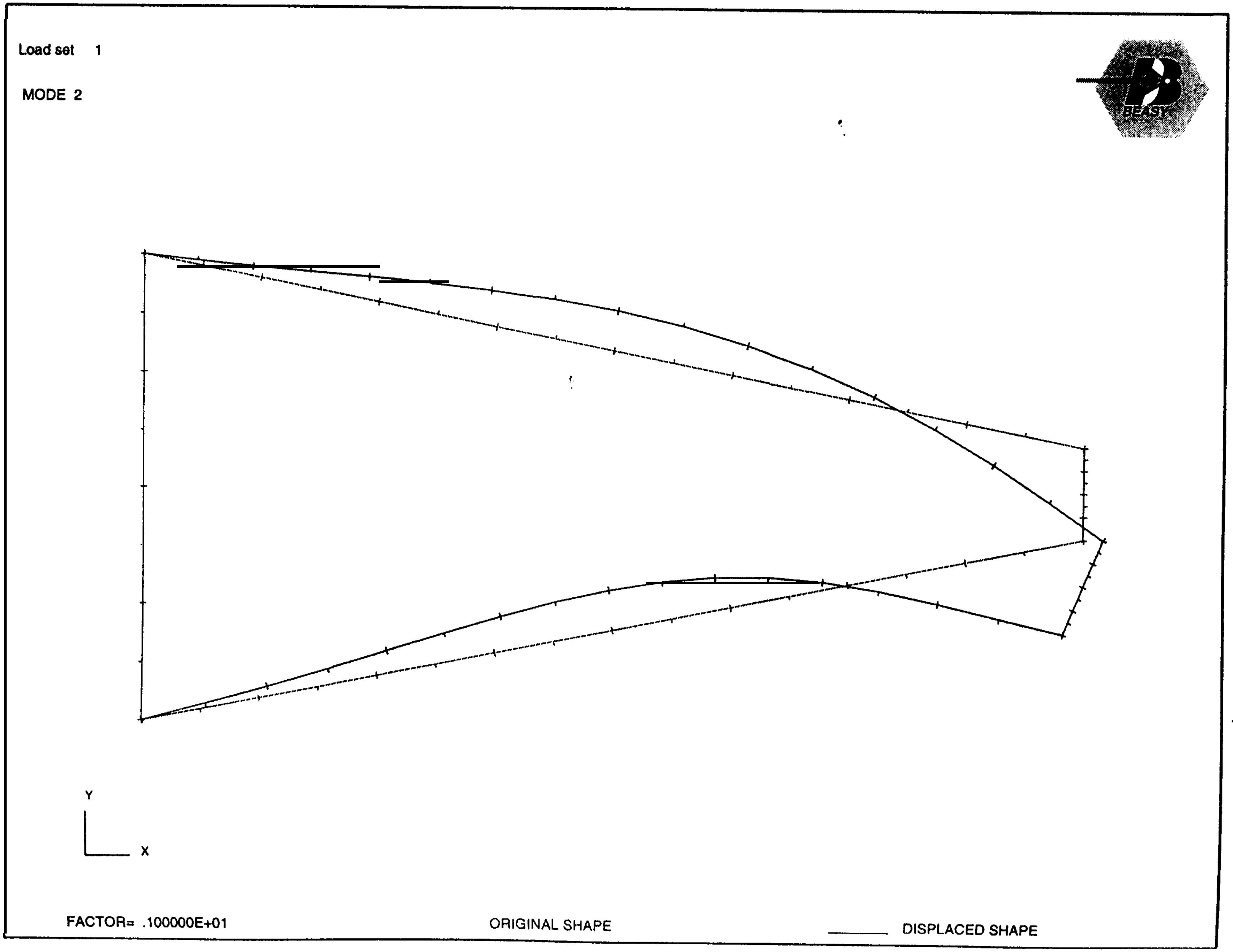

Load set 1
MODE 2
BEASY
Y
X
FACTOR= .100000E+01
ORIGINAL SHAPE
DISPLACED SHAPE

Fig (7.2)

Fig (7.3)

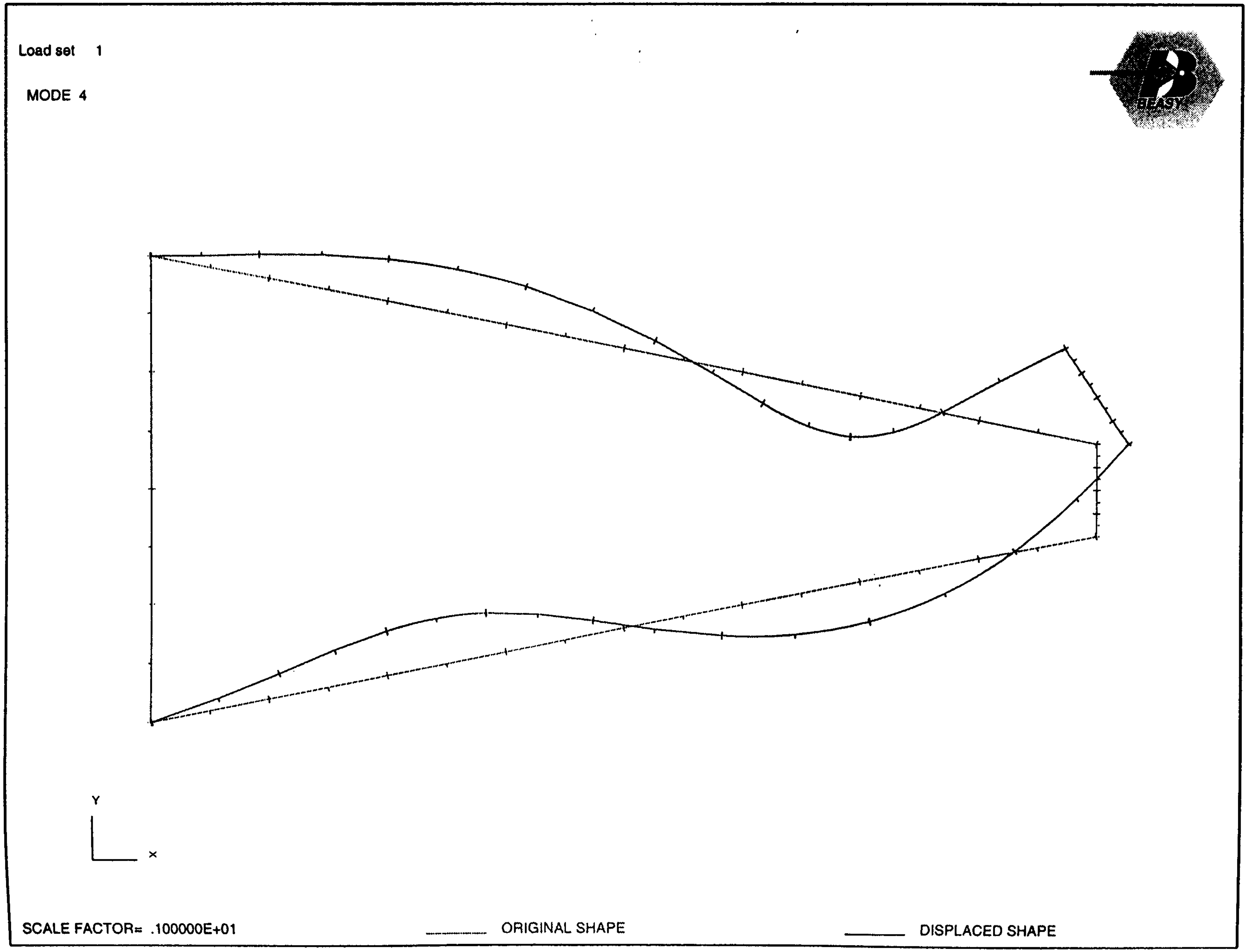
Load set 1
MODE 4
BEASY
Y
X
SCALE FACTOR= .100000E+01
ORIGINAL SHAPE
DISPLACED SHAPE

Fig (7.3)

Fig(2.4)

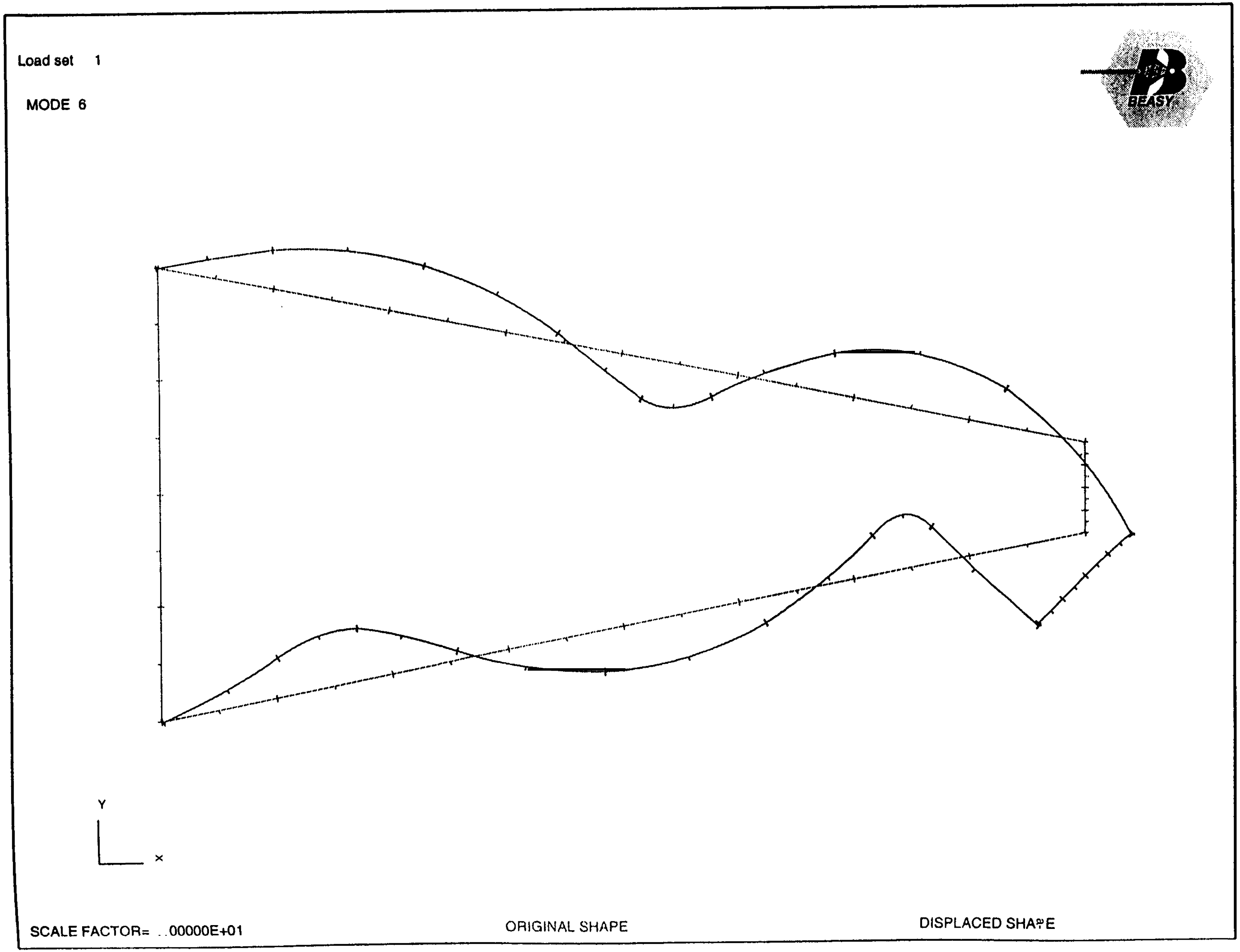

Load set 1
MODE 6
BEASY
Y
x
SCALE FACTOR= ..00000E+01
ORIGINAL SHAPE
DISPLACED SHAPE

Fig(2.4)

Fig (3)

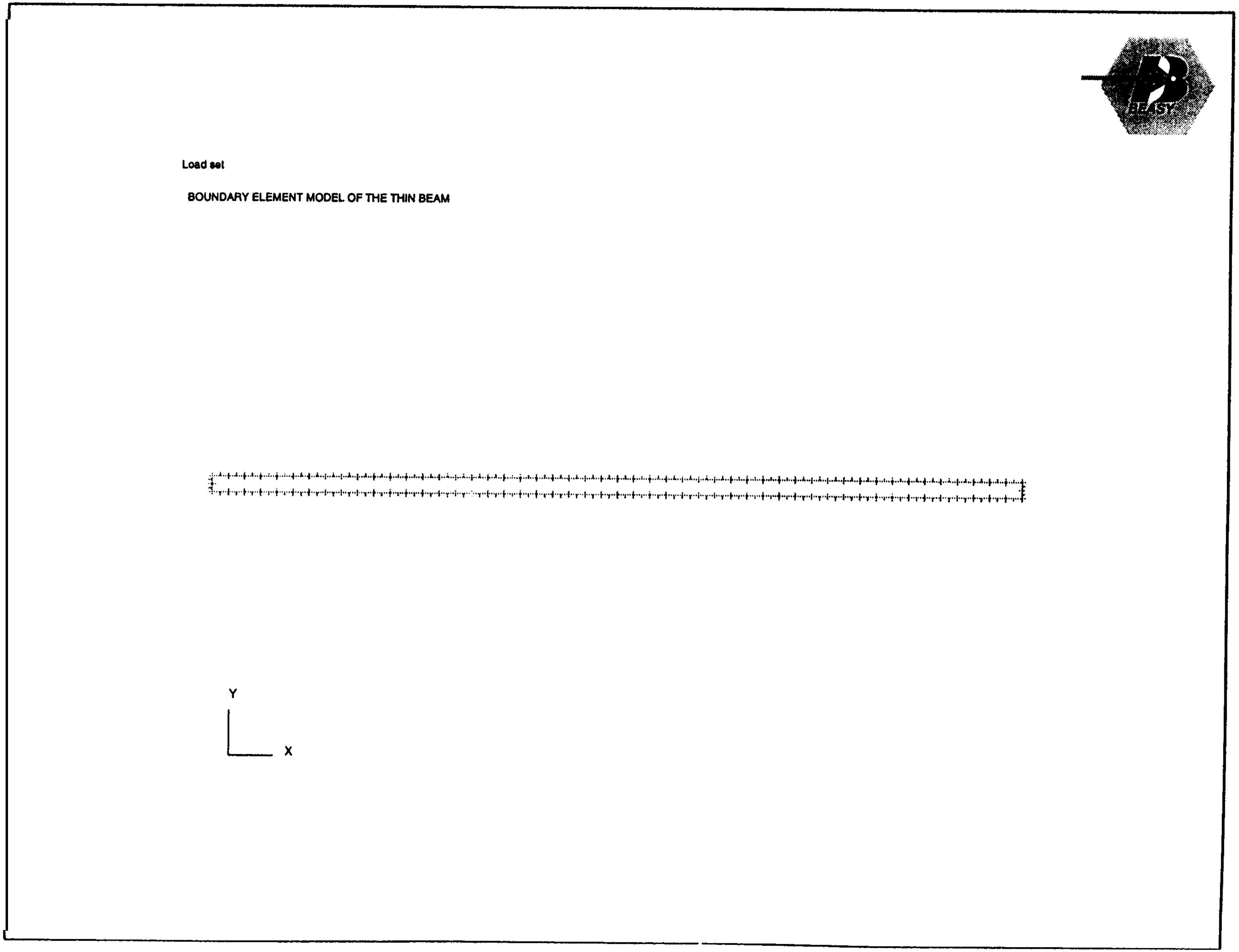

Fig (3)

Fig (4.1)

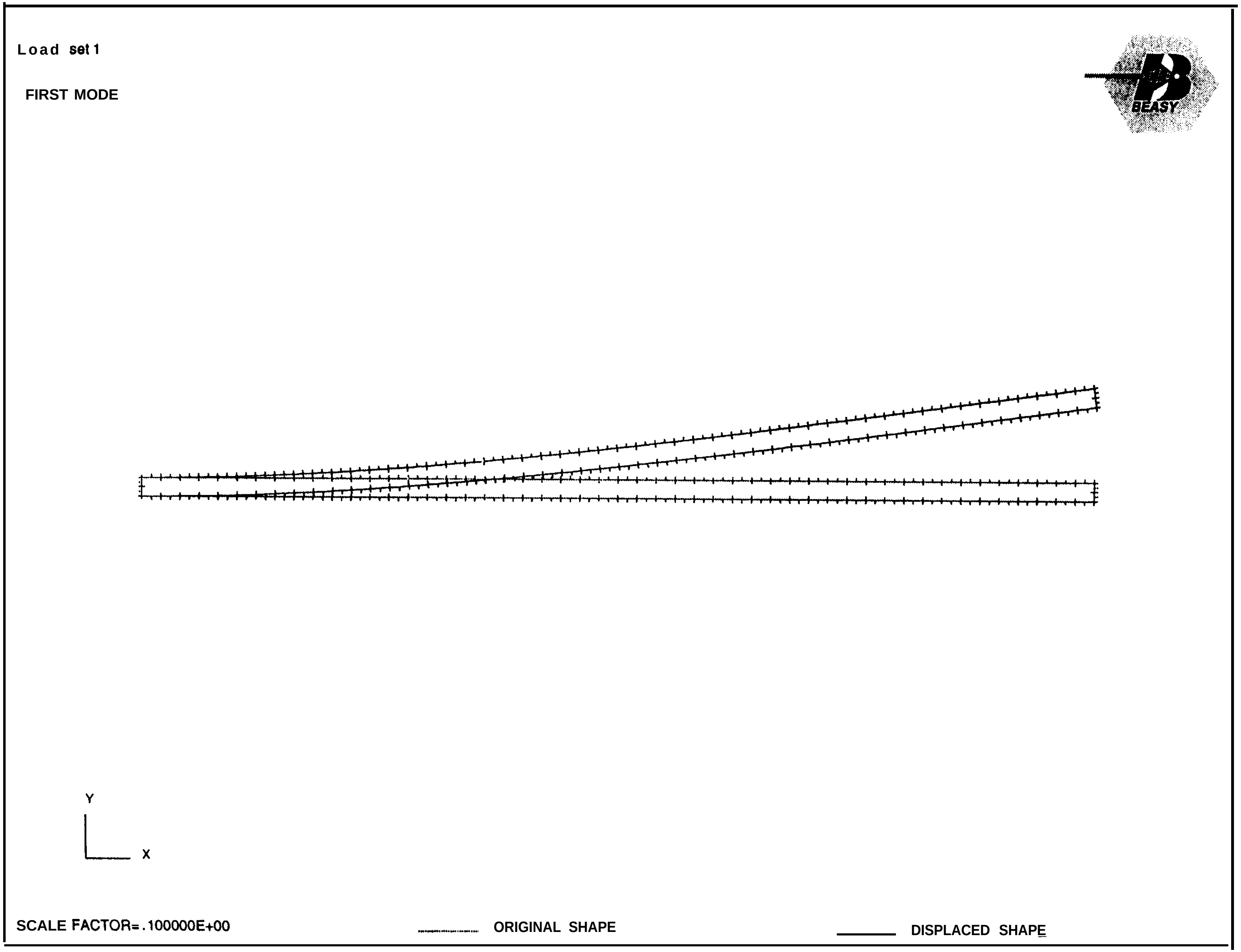

Load set 1
FIRST MODE
BEASY
Y
X
SCALE FACTOR=.100000E+00
ORIGINAL SHAPE
DISPLACED SHAPE

Fig (4.1)

Fig (4.2

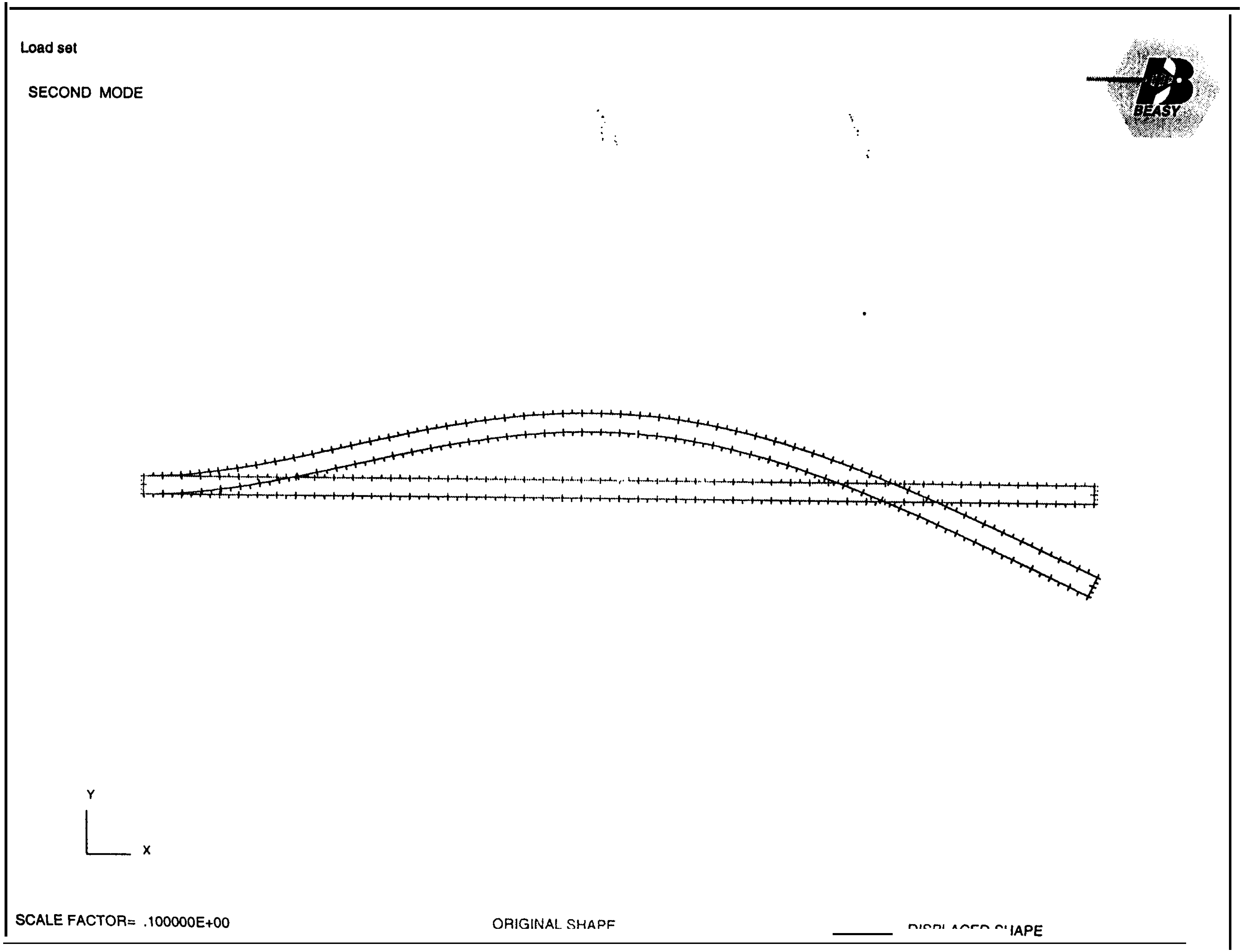

Load set
SECOND MODE
BEASY
Y
X
SCALE FACTOR= .100000E+00
ORIGINAL SHAPE
DISPLACED SHAPE

Fig (4.2)

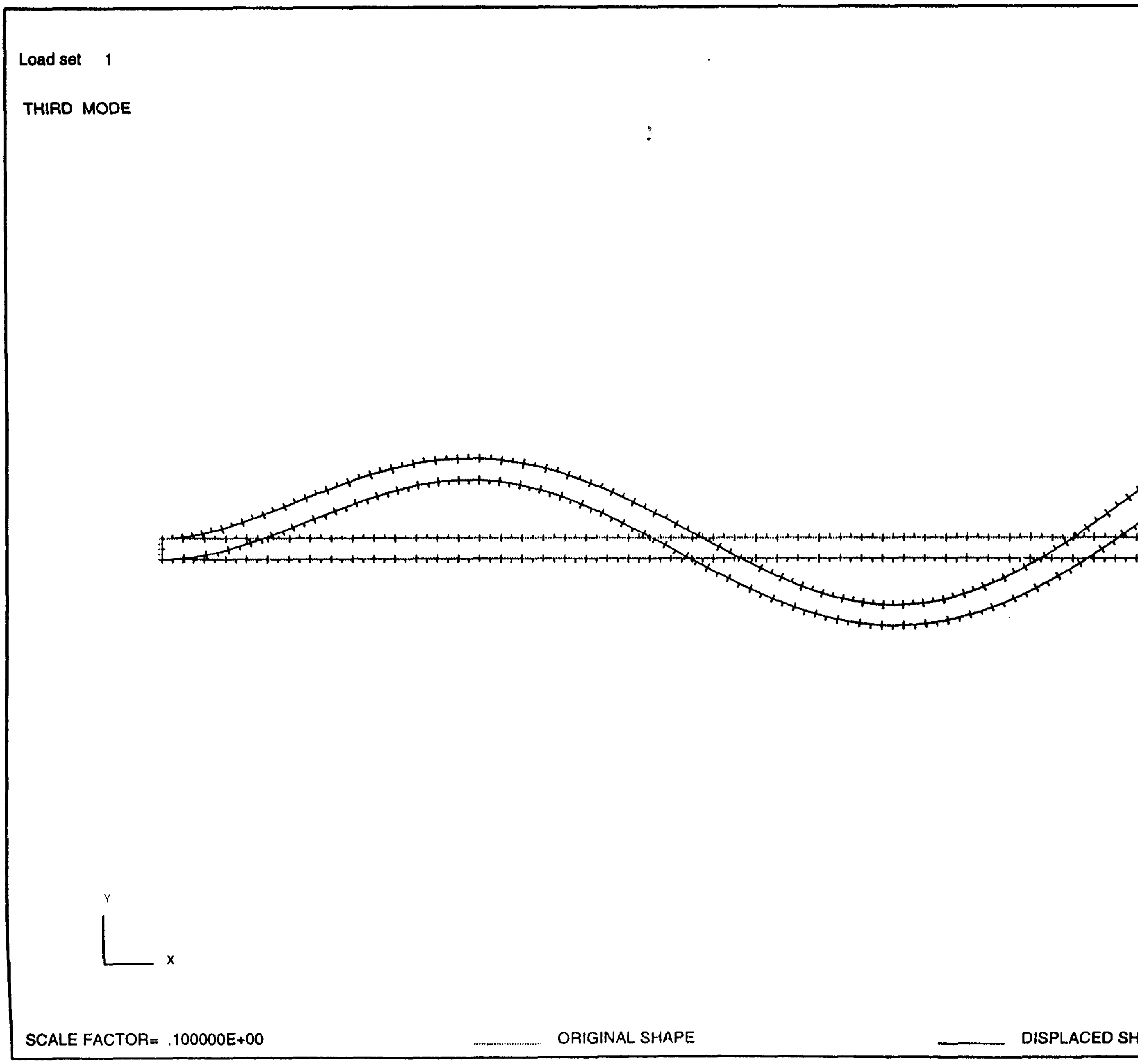
Load set 1
THIRD MODE
Y
X
SCALE FACTOR= .100000E+00
ORIGINAL SHAPE
DISPLACED SH

Fig (4.31)

Fig (4.4)

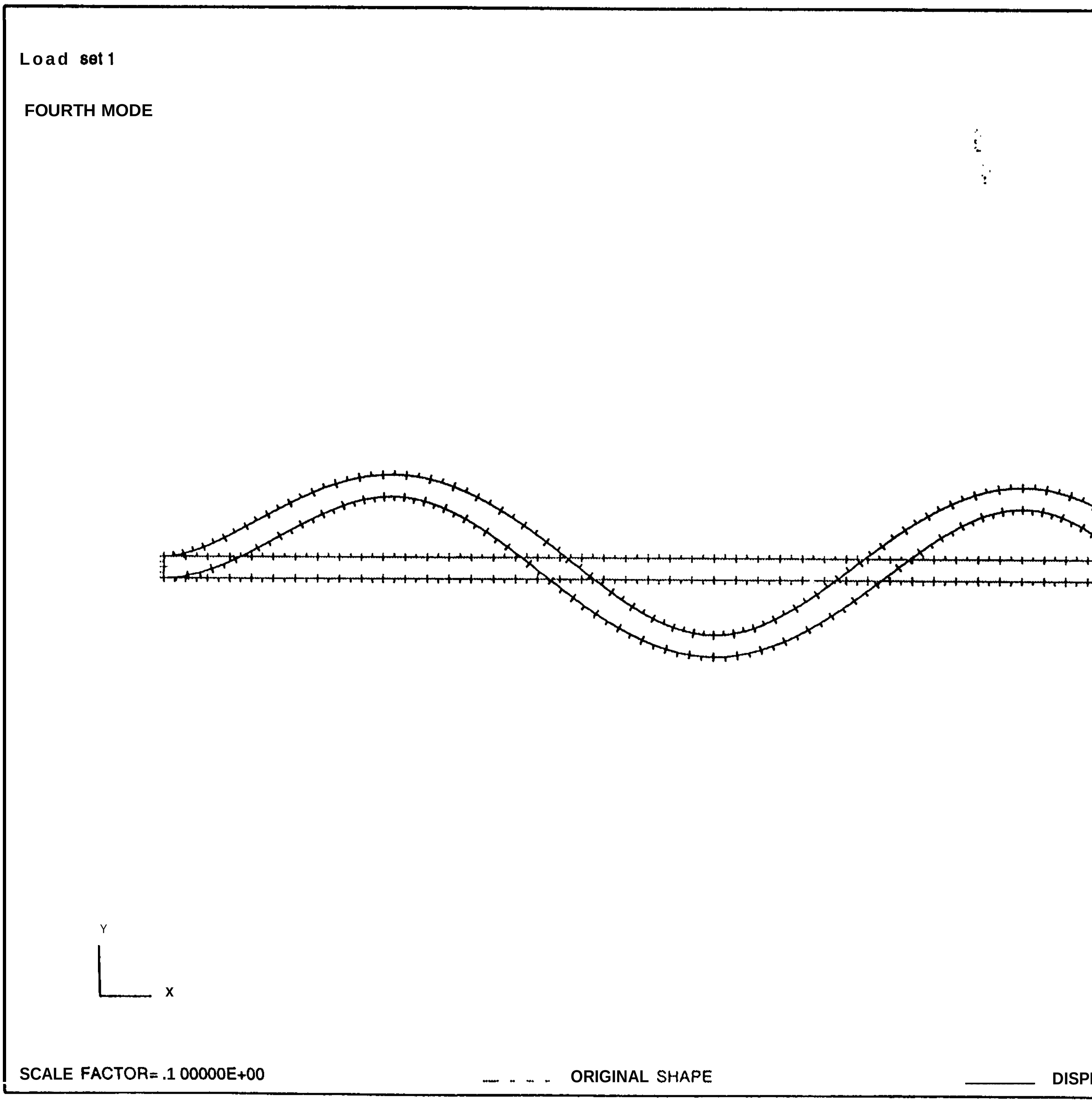

Load set 1
FOURTH MODE
Y
X
SCALE FACTOR=.1 00000E+00
ORIGINAL SHAPE
DISP

(5.1)

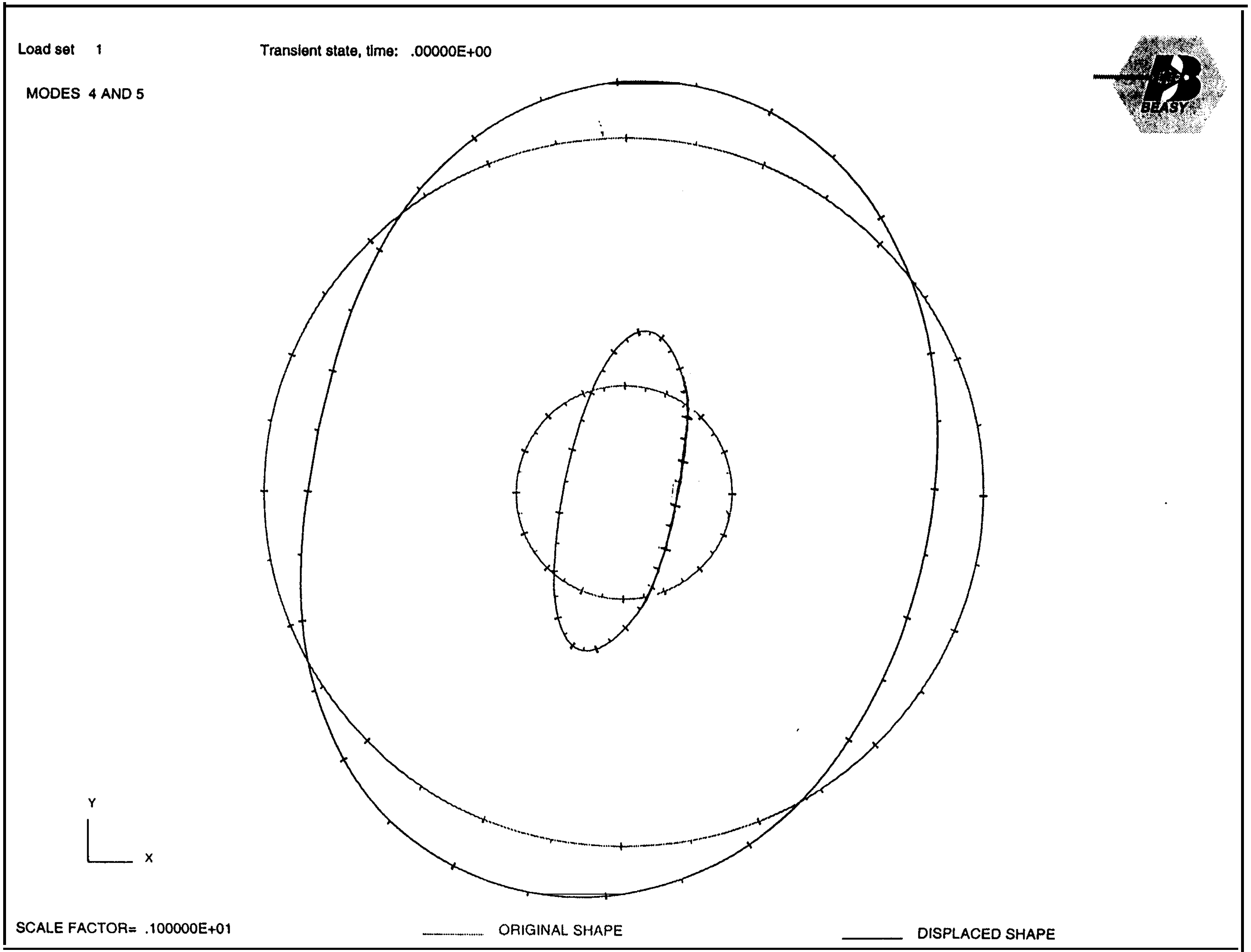
Load set 1
Transient state, time: .00000E+00
MODES 4 AND 5
BEASY
Y
X
SCALE FACTOR= .100000E+01
ORIGINAL SHAPE
DISPLACED SHAPE

Fig (5.1)

(5.2)

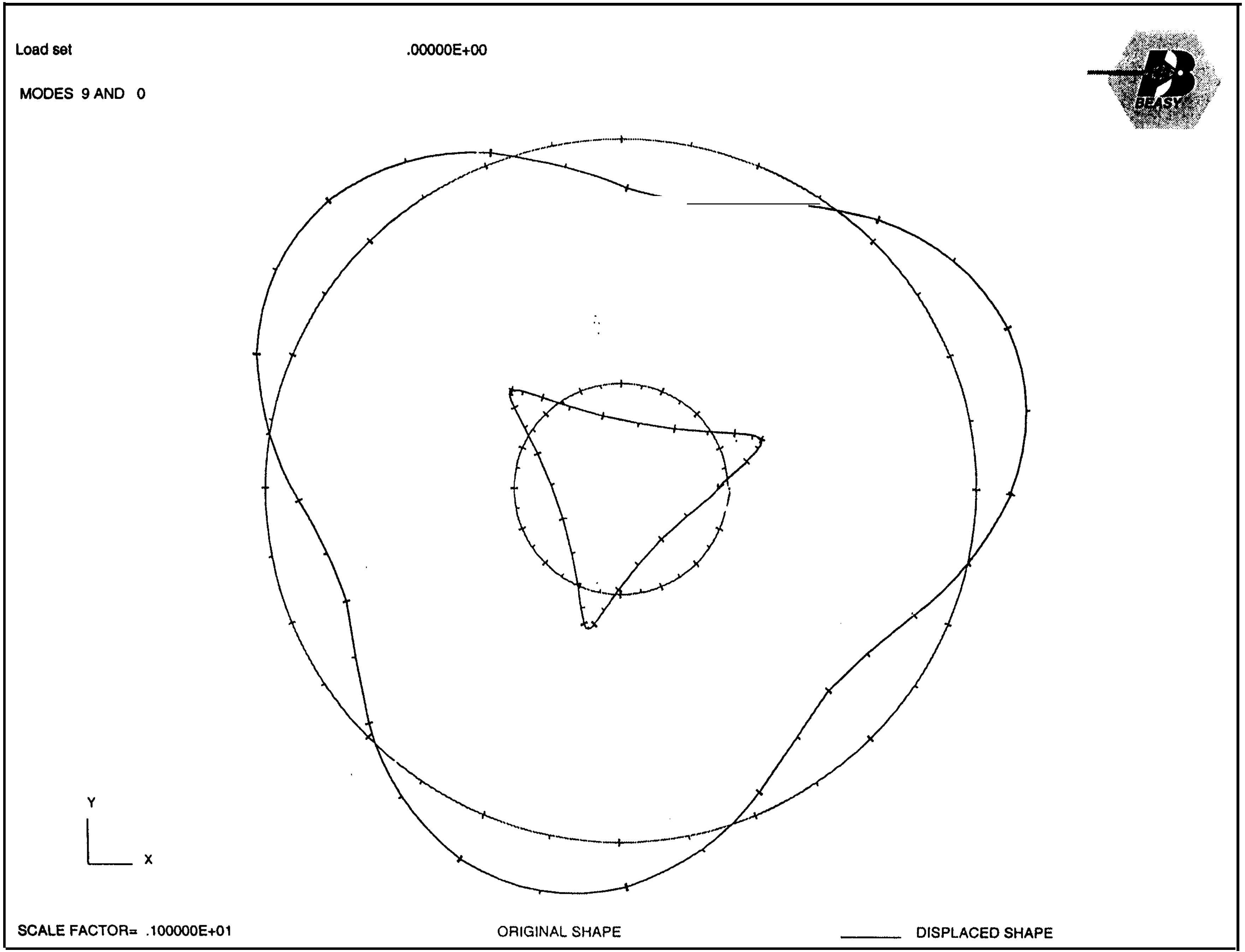

Load set
.00000E+00
MODES 9 AND 0
BEASY
Y
X
SCALE FACTOR= .100000E+01
ORIGINAL SHAPE
DISPLACED SHAPE

Figure (5.2)

(5.3)

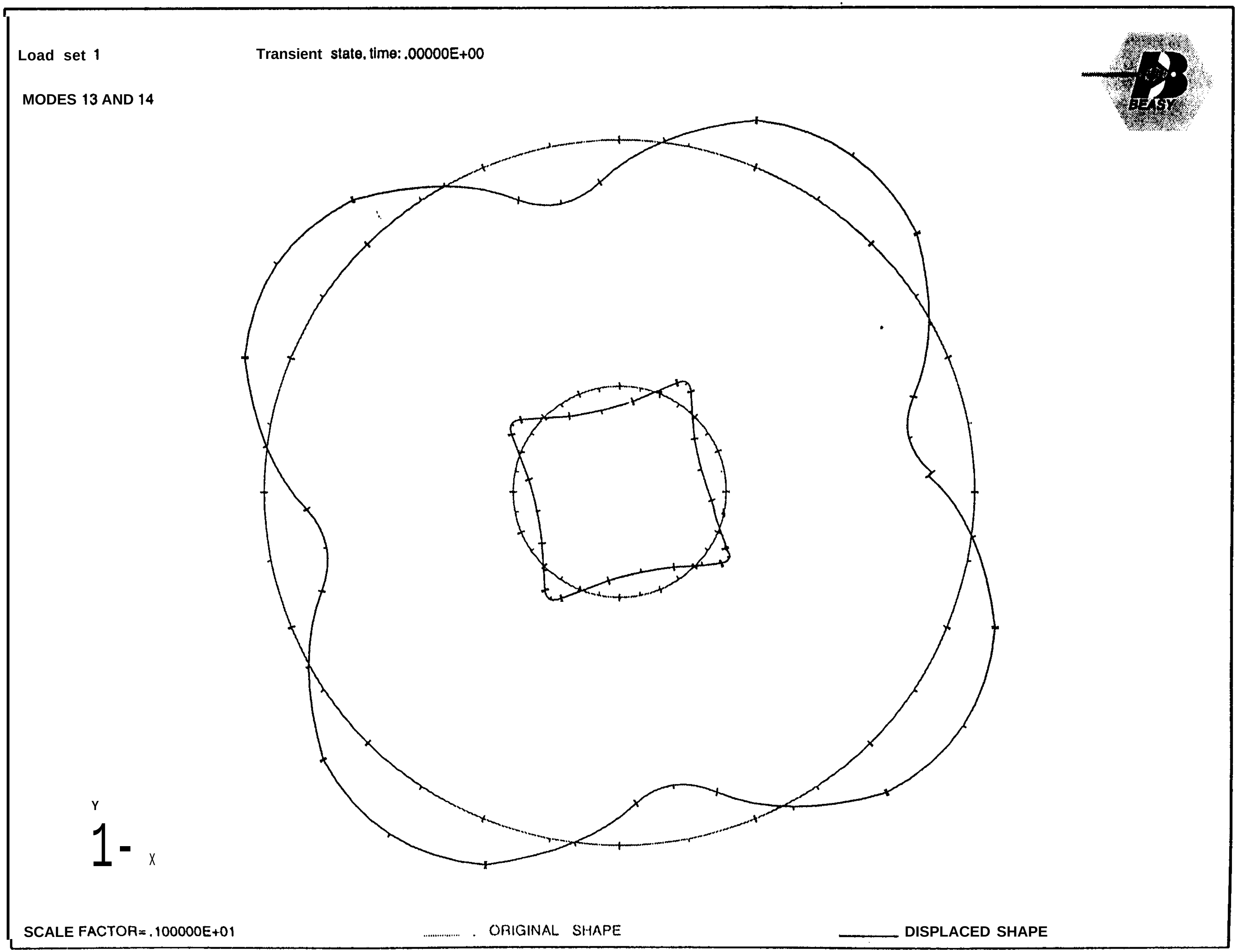

Load set 1
Transient state, time: .00000E+00
MODES 13 AND 14
BEASY
Y
1-
X
SCALE FACTOR= .100000E+01
ORIGINAL SHAPE
DISPLACED SHAPE

Fig (5.3)

Figure 6: Geometry of the micro hinge

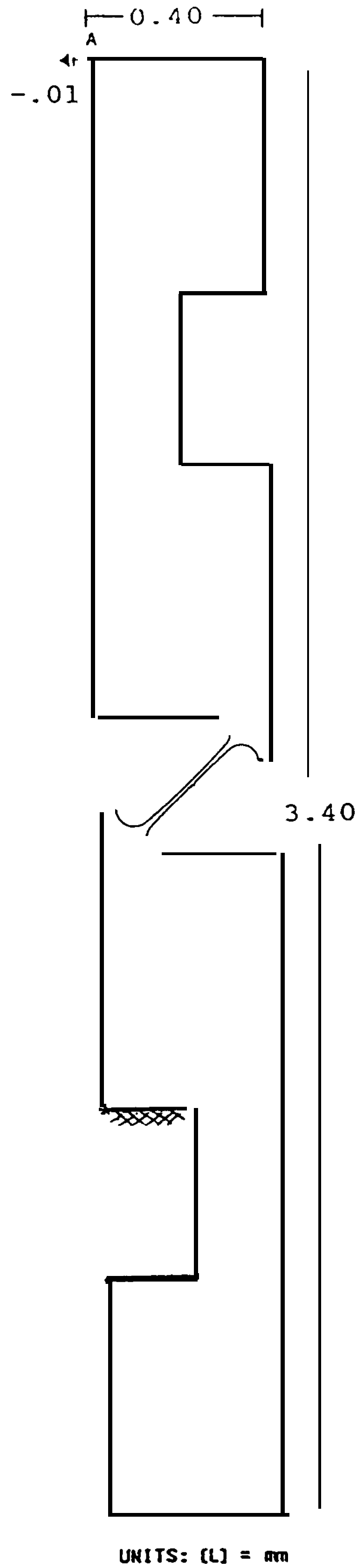

Fig(6)

Fig (7.1)

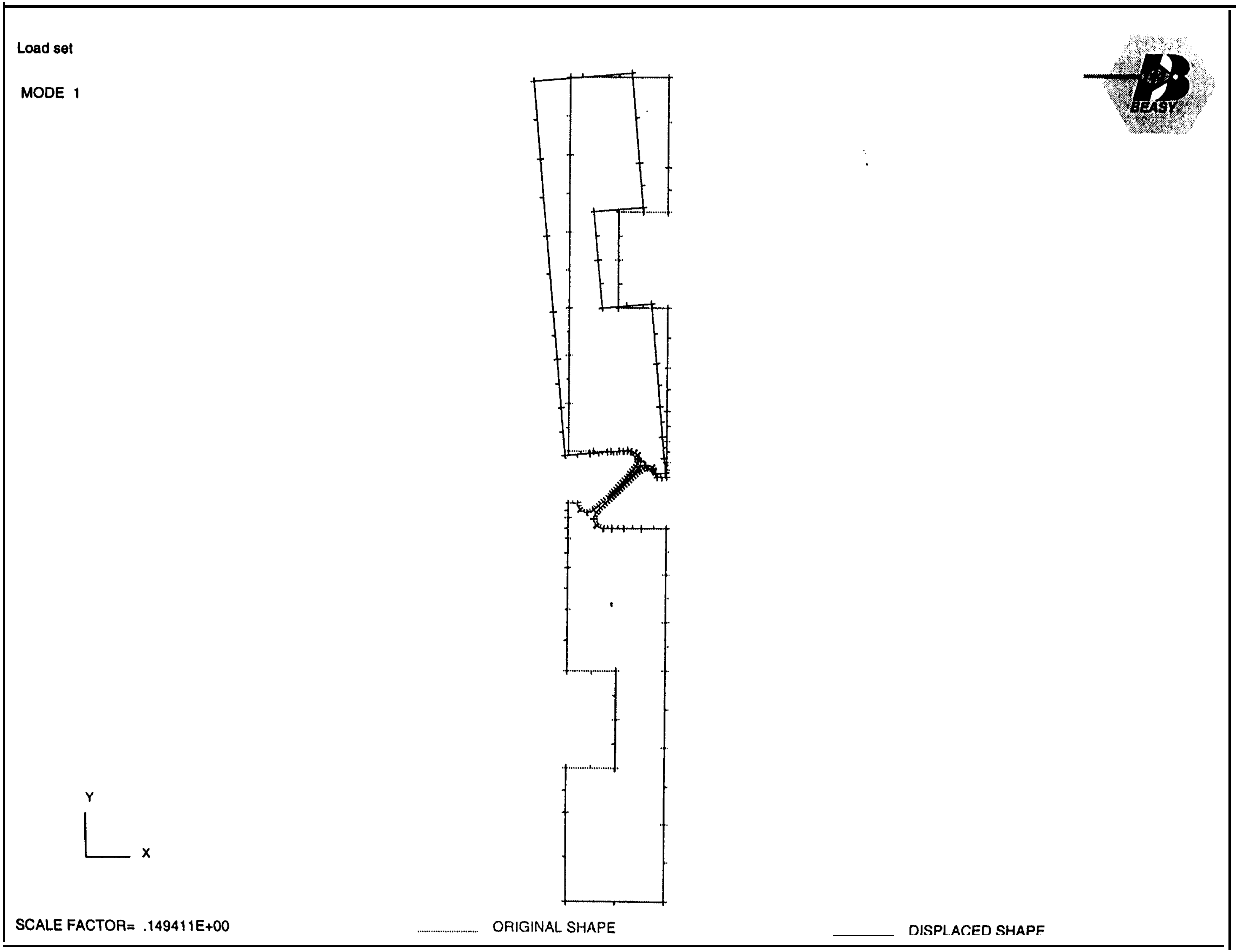

Load set
MODE 1
BEASY
Y
X
SCALE FACTOR= .149411E+00
ORIGINAL SHAPE
DISPLACED SHAPE

Fig (7.1)

Fig (7.7)


Load set 1
MODE 2
BEASY
Y
X
SCALE FACTOR= 20876E+00
ORIGINAL SHAPE
SHAPE

Fig (7.2)

Fig(7.31).

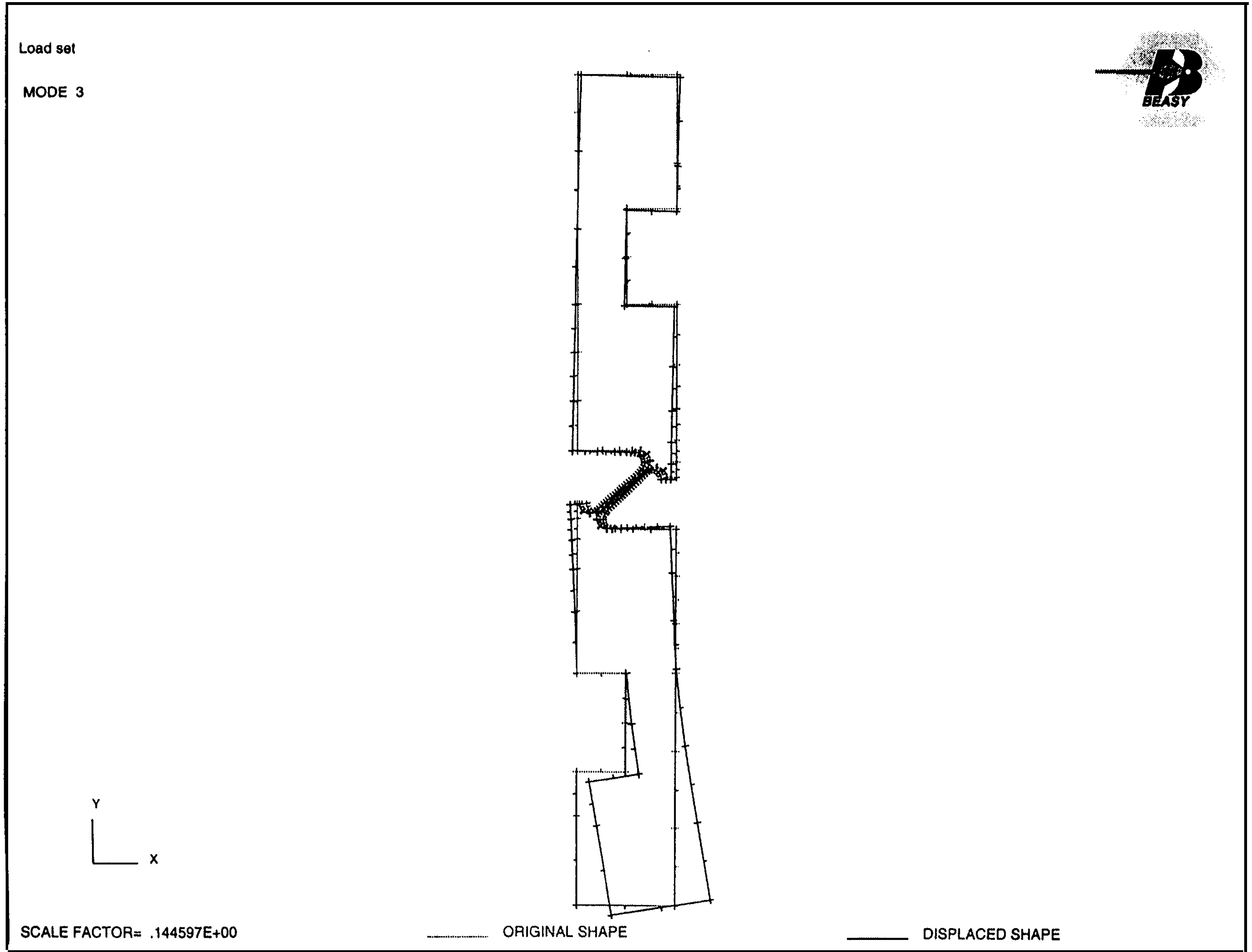

Fig(7.31)

Fig (7.41

Fig (7.4)

Load set

MODE 4

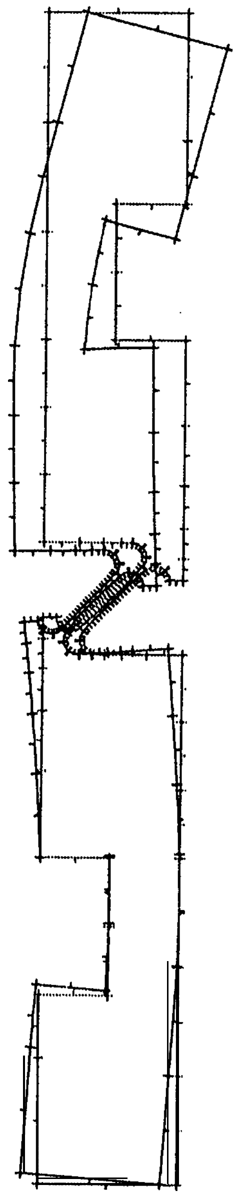

Y

X

= .110924E+00

ORIGINAL SHAPE

DISPLACED SHAPE

Fig(7.5)

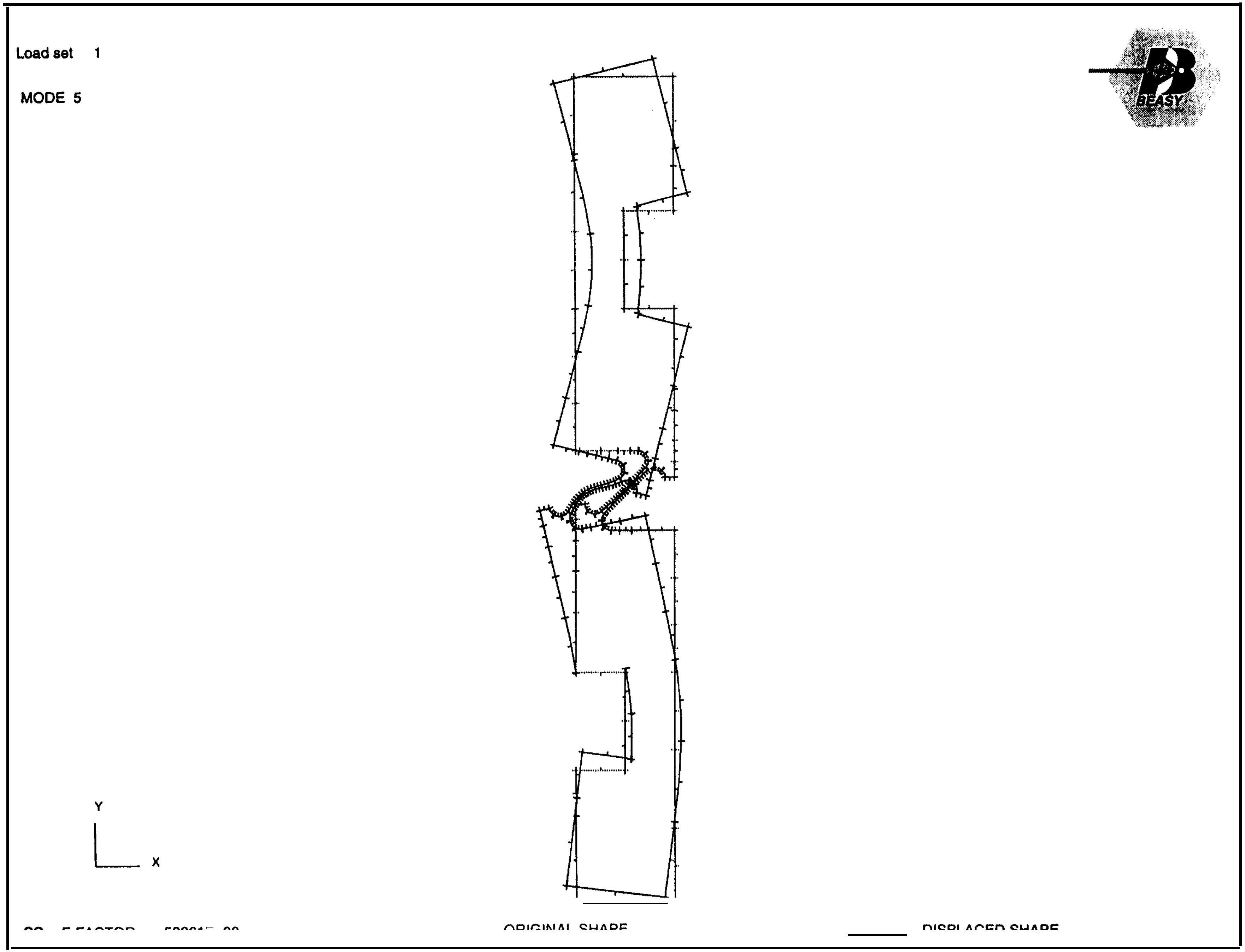

Fig(7.5)

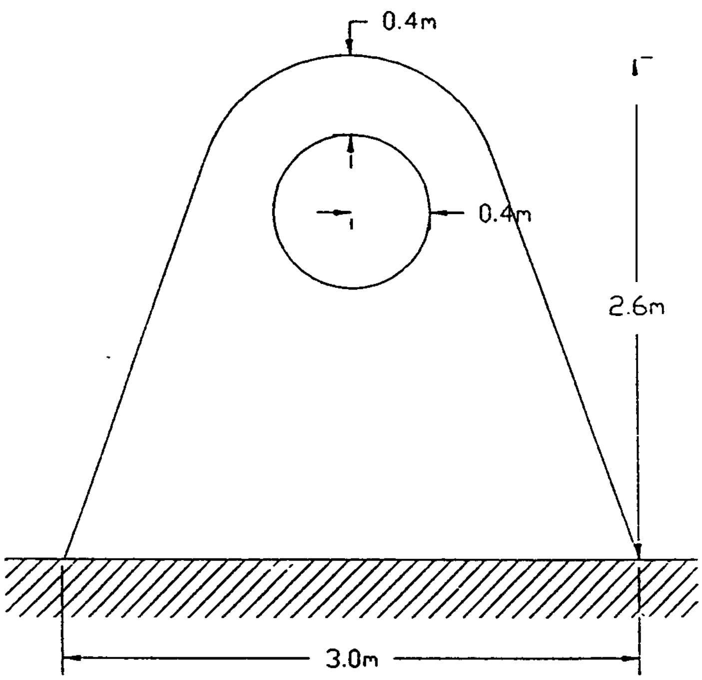

Figure 8.1: Geometry of the clamped lug

Fig (8.2)

BOUNDARY ELEMENT MODEL OF THE 3D LUG

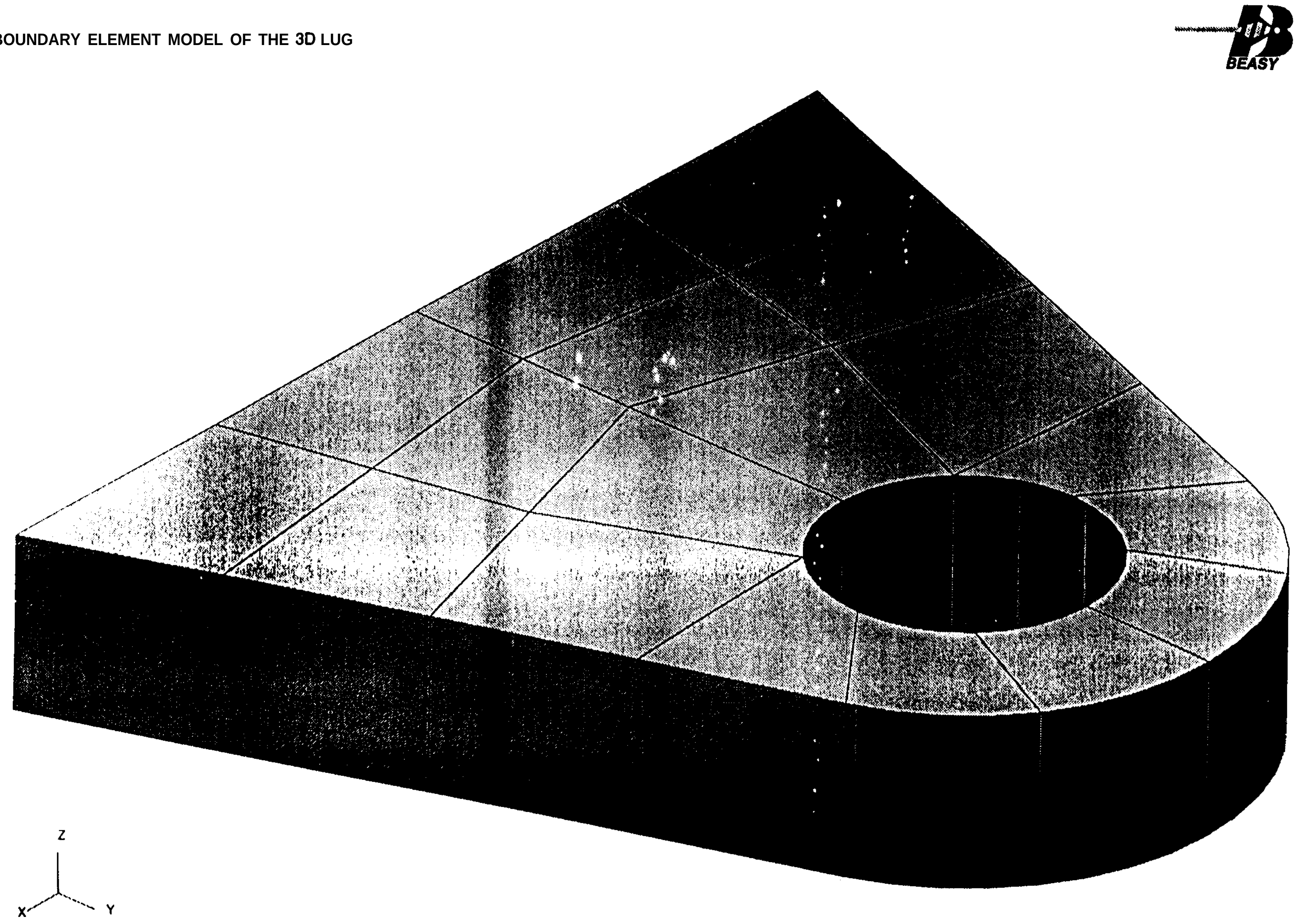

Fig(9.1)

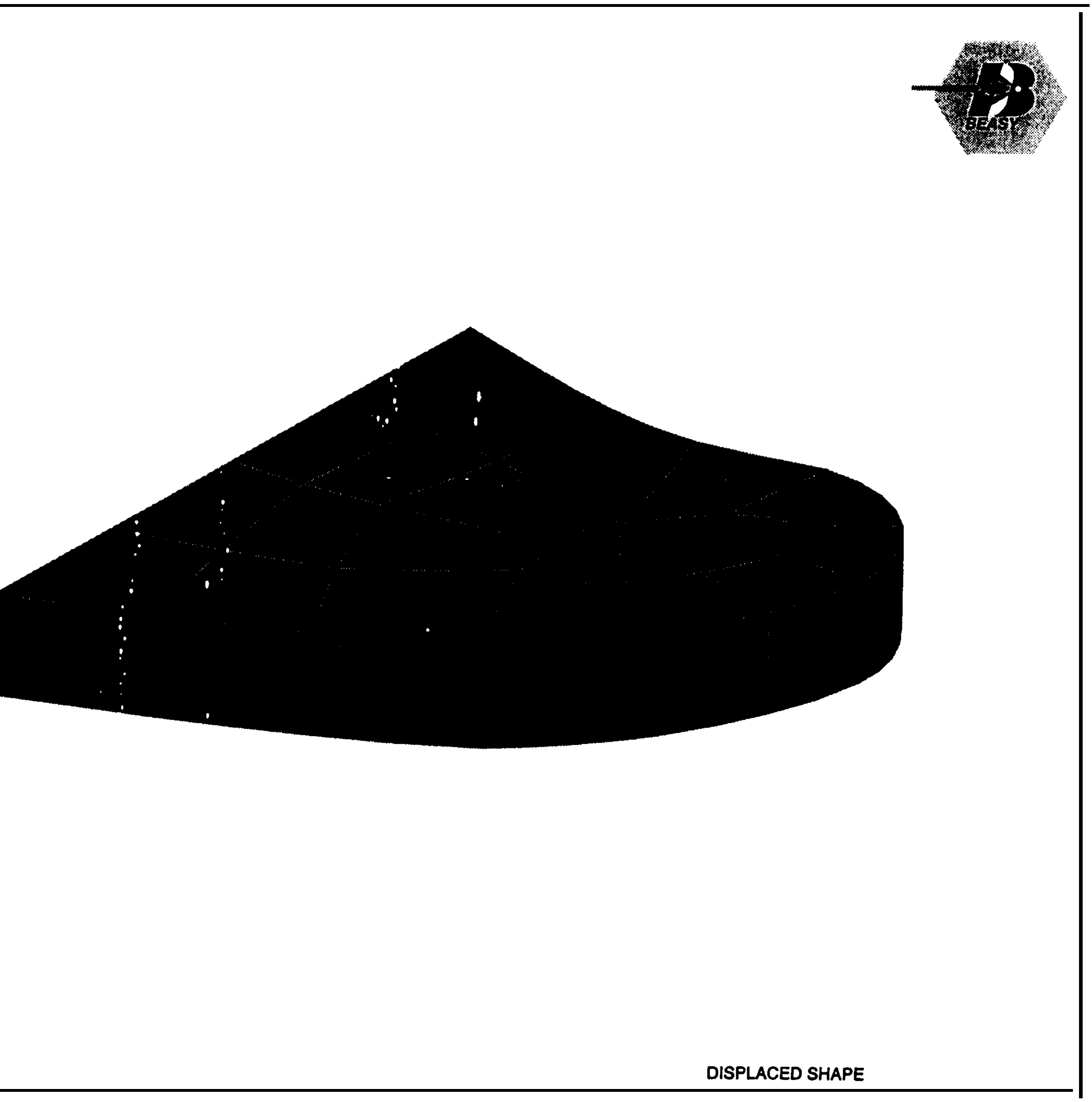

Fig(9.2

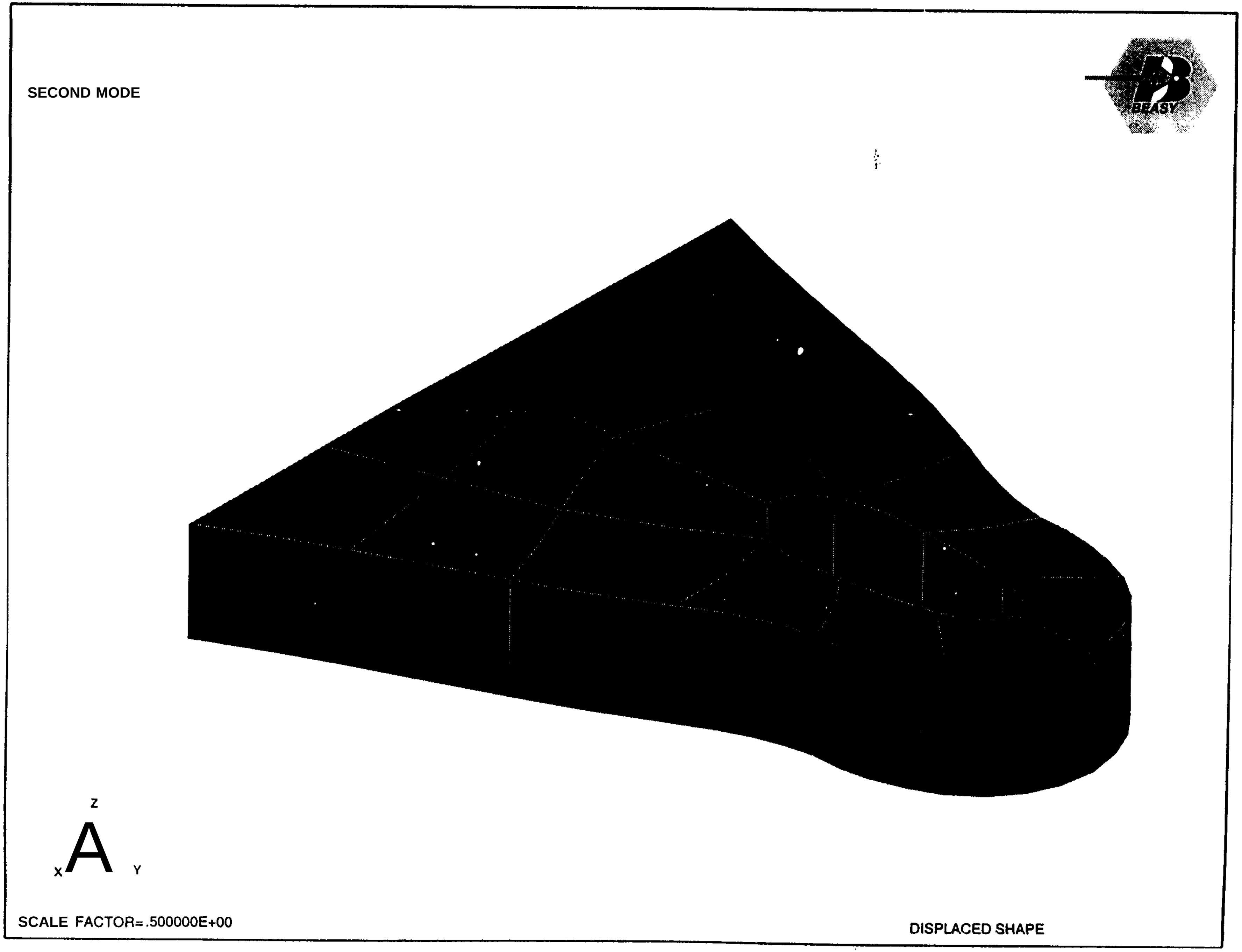
SECOND MODE
BEASY
Z
X
Y
SCALE FACTOR=.500000E+00
DISPLACED SHAPE

Fig 19.3,